Geophys. J. Int. (2009) **178,** 1555–1564 doi: 10.1111/j.1365-246X.2009.04239.x

On establishing the accuracy of noise tomography travel-time measurements in a realistic medium

Victor C. Tsai

Department of Earth and Planetary Sciences, Harvard University, Cambridge, MA 02138, *USA. E-mail: vtsai@post.harvard.edu*

Accepted 2009 May 4. Received 2009 April 16; in original form 2009 January 19

SUMMARY

It has previously been shown that the Green's function between two receivers can be retrieved by cross-correlating time series of noise recorded at the two receivers. This property has been derived assuming that the energy in normal modes is uncorrelated and perfectly equipartitioned, or that the distribution of noise sources is uniform in space and the waves measured satisfy a high frequency approximation. Although a number of authors have successfully extracted travel-time information from seismic surface-wave noise, the reason for this success of noise tomography remains unclear since the assumptions inherent in previous derivations do not hold for dispersive surface waves on the Earth. Here, we present a simple ray-theory derivation that facilitates an understanding of how cross correlations of seismic noise can be used to make direct travel-time measurements, even if the conditions assumed by previous derivations do not hold. Our new framework allows us to verify that cross-correlation measurements of isotropic surface-wave noise give results in accord with ray-theory expectations, but that if noise sources have an anisotropic distribution or if the velocity structure is non-uniform then significant differences can sometimes exist. We quantify the degree to which the sensitivity kernel is different from the geometric ray and find, for example, that the kernel width is period-dependent and that the kernel generally has non-zero sensitivity away from the geometric ray, even within our ray theoretical framework. These differences lead to usually small (but sometimes large) biases in models of seismic-wave speed and we show how our theoretical framework can be used to calculate the appropriate corrections. Even when these corrections are small, calculating the errors within a theoretical framework would alleviate fears traditional seismologists may have regarding the robustness of seismic noise tomography.

Key words: Surface waves and free oscillations; Seismic tomography; Theoretical seismology; Wave propagation; Crustal structure.

1 INTRODUCTION

In 2001, Lobkis & Weaver (2001) showed that the cross-correlation of signals from two receivers in a diffuse acoustic field yields the Green's function between the two receivers. They provided two plausibility arguments and a complete derivation of this property, all relying at least partially on the definition of a diffuse field as having uncorrelated and random modal amplitudes with equal variances, or alternatively that the energy in normal modes is uncorrelated and perfectly equipartitioned. Since this initial derivation, other derivations of the 'noise-correlation' property have been made under different assumptions. Using a reciprocity theorem, Wapenaar (2004) and Wapenaar *et al.* (2006) have shown that the same property holds for a general elastodynamic, inhomogeneous medium if the noise sources are numerous, well distributed and uncorrelated. Using a stationary-phase approximation, Snieder (2004) and Snieder *et al.* (2006) have also demonstrated that the property holds for a uniform-velocity medium with locally isotropic noise, and that equipartitioning of modal energy is not required. It has also recently been pointed out by a number of authors (Chavez-Garcia & Luzon 2005; Chavez-Garcia *et al.* 2005; Roux *et al.* 2005; Nakahara 2006; Sanchez-Sesma & Campillo 2006; Sanchez-Sesma *et al.* 2006) that the essential points of the noise correlation property have been known since the seminal work of Eckart (1953), Aki (1957), Claerbout (1968) and Cox (1973), and that the property has simply been rediscovered in a new context. All derivations of the 'noise correlation' property find that under certain favourable conditions, the Green's function between two stations can be obtained from the cross correlation of noise.

The existence of this noise-correlation property has led a number of authors to apply the idea to a variety of physical systems, including the Earth. By cross-correlating time series of seismic coda (Campillo & Paul 2003) or ambient seismic noise (Shapiro & Campillo 2004), these initial applications demonstrated that a time series resembling the Green's function can be obtained from real seismic noise and moreover that path-average seismic velocities measured using noise-correlation techniques agree well with those measured using traditional earthquake-based approaches. More

recently, numerous studies have utilized multiple station–station pairs to create regional models of Rayleigh-wave group and phase velocity (e.g. Sabra *et al.* 2005; Shapiro *et al.* 2005; Yao *et al.* 2006; Benson *et al.* 2007; Cho *et al.* 2007; Yang *et al.* 2007). Whereas noise-correlation tomography offers several advantages over traditional surface-wave techniques, most notably independence from earthquake occurrence and the ability to use shorter period waves, the Earth does not fully comply with the assumptions inherent in the derivations described above and the implications of this fact should be understood. Specifically, in the Earth, velocity is not uniform, sources are not isotropically distributed and modal energy is not equipartitioned. In fact, strong directional dependence (and hence anisotropic distribution) of ambient noise sources has been partially characterized by Stehly *et al.* (2006) and Yang & Ritzwoller (2008). Yang & Ritzwoller (2008) show (using numerical simulations) that the error due to this dependence is often small. A number of authors (e.g. Derode *et al.* 2003; Larose *et al.* 2006; Yang & Ritzwoller 2008) have also shown with numerical or experimental simulations that a time series resembling the Green's function is often obtained through cross-correlation. However, much of the literature does not clearly distinguish between the ability to obtain a Green's function-like time series and the ability to make a meaningful travel-time measurement on it; moreover, the literature lacks a simple analytical approach to the problem of quantifying the effects of non-uniformity of velocities and noise sources in tomographic travel-time measurements. This gap in the current literature motivates this work.

In this work, we focus on understanding why it is possible to make travel-time measurements on direct arrivals of correlated noise even with a non-uniform distribution of noise sources, a non-uniform velocity structure and potentially dispersive waves. To achieve this goal, in Section 2.1, we first present a simple ray-theoretical derivation that explains the relationship between a standard cross-correlation measurement of noise and the ray-theoretical travel time between the pair of stations. Using this new approach, we can then evaluate the success of a travel-time measurement without resorting to numerical simulations. We are, thus, able to easily explore a variety of situations in which the success of these measurements is not clear *a priori* and furthermore give a quantitative assessment of the errors accrued. In Section 2.3, we then show that when noise sources are uniformly (isotropically) distributed and the medium has uniform velocities, our approach becomes approximately equivalent to a stationary-phase approach like that of Snieder (2004) and we therefore recover similar conclusions regarding the success of noise tomography applications. Under an infinite-frequency approximation, our results simplify considerably, allowing one to assess the validity of a travel-time measurement with virtually no computation. Finally, in Section 3, taking advantage of the new approach, we present a few examples that exemplify the types of issues that commonly arise and suggest a method of correcting for these (typically small but occasionally large) errors between the actual station–station travel time and the time measured by standard correlation measurements.

2 THEORETICAL DEVELOPMENT FOR NOISE CORRELATION MEASUREMENTS

2.1 An analytic description of the travel-time measurement of distributed noise

In this section, we provide a simple analysis of how the cross-correlation of noise recorded at two seismic stations can be used to make a meaningful travel-time measurement. In this analysis, we do not make the common assumptions of a uniform noise distribution, a uniform velocity medium, or equipartition of energy, but instead make assumptions that are perhaps more reasonable for the Earth. Specifically, we assume that there exist potentially frequency-dependent noise sources distributed in space with density $\rho_S(\boldsymbol{x}, \omega)$ (as a function of position $\boldsymbol{x}$ and at each frequency ω) that send waves along straight ray paths through a potentially dispersive medium and these sources are observed at each station x with travel time given by $\Delta t_x = \Delta x_{sx}/v_{avg-sx}$ where Δx_{sx} is the source–station distance and v_{avg-sx} is the average velocity along that path (at the given frequency). Whereas this ray-theoretical description is quite simplified, it follows similar assumptions of many traditional tomographic studies (e.g. Ritsema *et al.* 2004; Kustowski *et al.* 2008) that obtain very realistic velocity structures. All shortcomings of these studies, such as the lack of finite-frequency kernels (Montelli *et al.* 2004), lack of mode coupling (Li & Romanowicz 1995) and lack of ray curvature around velocity anomalies are also shortcomings of this work. The intention of this work is to highlight differences between noise tomography and traditional tomography, not to address issues common to both approaches. Since all comparisons are also done with respect to ray theory (e.g. in Section 3), errors due to known deficiencies of ray theory should be added to the errors discussed here (possibly resulting in a smaller net error).

We make the further assumption that, as in all other derivations of a noise-correlation property (e.g. Lobkis & Weaver 2001; Snieder 2004; Wapenaar 2004), the cross-correlation is performed over a sufficiently long time series that the cross-correlation is simply the sum of individual sinusoidal source terms, with all cross-terms cancelling out. A simple example of this is as follows. Let $C_{xy}(\Delta t)$ be the normalized cross-correlation between displacement seismograms $D(t)$ at points x and y as a function of traveltime delay Δt (This analysis applies to any component of the seismogram as long as the same component is used at both stations.). First, we consider the simple case of a deterministic wave source observed at point x with response given by $D(x, t) = \cos(\omega t + \phi)$, where ϕ is a constant phase delay and the same source observed with relative time delay Δt_d at y such that $D(y, t) = \cos[\omega (t - \Delta t_d) + \phi]$. For this single-source situation, then

$$\begin{aligned} C_{xy}(\Delta t, \omega) &= \frac{1}{T}\int_{-T}^{T} D(x,t)D(y,t+\Delta t)\,dt \\ &= \cos[\omega(\Delta t - \Delta t_d)] \\ &\quad - \frac{\sin[2\omega T]}{2\omega T}\cos[\omega(\Delta t - \Delta t_d) + 2\phi] \\ &\approx \cos[\omega(\Delta t - \Delta t_d)], \end{aligned} \tag{1}$$

where the last approximation is valid as long as $T \gg 1/\omega$, that is the correlation time T is sufficiently long, and holds for arbitrary phase shift ϕ. If ϕ is allowed to vary only over timescales longer than Δt, we observe that the same result holds by breaking the integral into shorter pieces. Thus, we find that a 'noise source' (with ϕ varying stochastically over long timescales) observed through cross correlation is identical to a deterministic source of the same ω and Δt_d. We further observe that adding stochastic terms $N_1(t)$ and $N_2(t)$ to $D(x, t)$ and $D(y, t)$, respectively, so that the displacement responses are given by $D(x, t) = \cos(\omega t) + N_1(t)$ and $D(y, t) = \cos[\omega(t - \Delta t_d)] + N_2(t)$, does not affect the cross-correlation response as long as N_1 and N_2 are uncorrelated with each other and uncorrelated with $\cos(\omega t)$. As stated earlier, these facts have been shown by many previous authors and we refer the reader to those works for further discussion of the assumptions. It should be noted

that Δt_d should be interpreted as the travel-time delay between when the noise source is observed at point x and point y and can be expressed as

$$\Delta t_d = \Delta t_y - \Delta t_x = \frac{\Delta x_{sy}}{v_{\mathrm{avg}-sy}} - \frac{\Delta x_{sx}}{v_{\mathrm{avg}-sx}}. \tag{2}$$

When $D(x,t)$ and $D(y,t)$ are given by a sum of sinusoids at varying Δt_d, then eq. (1) immediately generalizes to a sum. For example, if there are two equal cosine source terms, with travel-time delay of Δt_{d1} and Δt_{d2}, respectively, then the assumption of cancelling cross-terms leads to

$$C_{xy}(\Delta t, \omega) = \cos[\omega(\Delta t - \Delta t_{d1})] + \cos[\omega(\Delta t - \Delta t_{d2})]. \tag{3}$$

If sources are distributed with a distribution of travel-time delays and have unequal amplitude or prevalence, then cross-terms still cancel and this generalizes further to give

$$C_{xy}(\Delta t, \omega) = \int \rho(\Delta t_d, \omega) \cos[\omega(\Delta t - \Delta t_d)] d\Delta t_d, \tag{4}$$

where $\rho(\Delta t_d, \omega)$ is the 'density' of noise sources with travel-time delay Δt_d and frequency ω. Considering the effects of a source having a given amplitude and non-infinite duration in eq. (1) shows that this density function should weight source amplitude variations by a factor of amplitude squared whereas weighting source prevalence linearly with total source duration. For example, if one noise source had an amplitude three times that of a second source, the second source would need to contribute over a duration nine times longer to have an equal contribution to $\rho(t, \omega) \equiv \rho(\Delta t_d, \omega)$. Eq. (4) has a very simple interpretation. The cross-correlation response (at a given frequency) is simply the weighted sum of individual noise source terms that accounts for the prevalence of each source. In this analysis, attenuation is not explicitly considered but could be accounted for by a suitable re-definition of $\rho(t, \omega)$.

Before turning to the issue of how to determine $\rho(t, \omega)$, we discuss one final point regarding a time-windowed response. One is often interested only in a small segment of the cross-correlation (e.g. around a packet of waves near the group velocity) rather than the whole cross-correlation function. In these cases, it is standard practice to zero the data outside of the time window expected to contribute. This windowing procedure is exactly equivalent to down-weighting the sources contributing at these travel-time delays and we therefore express a windowed cross-correlation measurement as

$$\begin{aligned} C_{xy}(\Delta t, \omega, W) &= \int W(\Delta t_d) \rho(\Delta t_d, \omega) \cos[\omega(\Delta t - \Delta t_d)] d\Delta t_d \\ &= Re\left[e^{i\omega \Delta t} \int W(t) \rho(t, \omega) e^{-i\omega t} \, dt \right], \end{aligned} \tag{5}$$

where $W(t)$ is the chosen time window function.

If one knows $\rho(t, \omega)$ then one can calculate the windowed cross-correlation response using eq. (5), so it only remains to determine the relationship between the density of noise sources as a function of traveltime delay, $\rho(t, \omega)$, and the density of noise sources in physical space, $\rho_S(\boldsymbol{x}, \omega)$. One can abstractly define this relationship as

$$\int_{\Delta t_1}^{\Delta t_2} \rho(\Delta t, \omega) \, d\Delta t = \int_{\boldsymbol{x}, \Delta t_1 \le \Delta t \le \Delta t_2} \rho_S(\boldsymbol{x}, \omega) |\, d\boldsymbol{x}|. \tag{6}$$

That is, the density of sources in a certain travel-time delay interval is simply the density of sources in space integrated over all spatial points with a travel-time delay within the given range. In certain important cases that will be discussed in Sections 2.2 and 2.5, the spatial density can be parametrized simply with a single scalar variable, ξ, such that one can explicitly write $\xi(\boldsymbol{x})$ as a scalar field and a constant value of ξ implies constant Δt. In this case, we similarly define

$$\int_{\xi_1}^{\xi_2} \rho_S(\xi, \omega) \, d\xi = \int_{\boldsymbol{x}, \xi_1 \le \xi \le \xi_2} \rho_S(\boldsymbol{x}, \omega) |\, d\boldsymbol{x}| \tag{7}$$

and one can then explicitly solve for $\rho(t, \omega)$ by noting

$$\begin{aligned} \int_{\Delta t_1}^{\Delta t_2} \rho(\Delta t, \omega) \, d\Delta t &= \int_{\xi(\Delta t_1)}^{\xi(\Delta t_2)} \rho_S(\xi, \omega) |d\xi| \\ &= \int_{\Delta t_1}^{\Delta t_2} \rho_S(\xi(\Delta t), \omega) \cdot \left| \frac{d\xi(\Delta t)}{d\Delta t} \right| d\Delta t \end{aligned} \tag{8}$$

so that

$$\rho(t, \omega) = \rho_S(\xi(t), \omega) \cdot \left| \frac{d\xi(t)}{dt} \right| = \rho_S(\xi, \omega) \cdot \left| \frac{dt(\xi)}{d\xi} \right|^{-1}. \tag{9}$$

In eq. (9), $t(\xi)$ is the travel-time delay and is thus given by eq. (2) for each source point. In some instances, eq. (9) can be multi-valued, in which case one should sum the multi-valued contributions to ρ at each value of t.

We have now described an analytic procedure (eq. 5) for measuring a windowed cross-correlation response for a given source distribution $\rho_S(\xi, \omega)$ and a given velocity distribution, through the dependence of eq. (2). A standard travel-time measurement (e.g. Ekström *et al.* 1997) of this cross-correlation is the phase lag of the cross-correlation peak and is therefore given by

$$\tau(\omega) = \frac{1}{\omega} \left\{ \phi \left[\int W(t) \rho(t, \omega) e^{i\omega t} \, dt \right] + 2\pi N \right\}, \tag{10}$$

where ϕ is the phase (defined from 0 to 2π) of the complex signal and $2\pi N$ is the well-known phase ambiguity. This phase delay $\tau(\omega)$ (which has units of time) is the one measured by seismic noise tomography applications (irrespective of whether phase velocity or group velocity measurements are initially made). Differences between this quantity and the desired phase travel time are addressed later.

2.2 Application to far-field surface waves

When this new framework is applied to far-field surface waves, the description is especially simple. For surface waves, depth structure is integrated out so that the noise sources are effectively distributed in two dimensions (e.g. parametrized as a function of distance and azimuth). With the additional far-field assumption, sources are assumed to be along a circle infinitely far away and an obvious natural scalar-variable parametrization is to set $\xi = \theta$ where θ is the azimuth of the source relative to the station–station line (see Fig. 1). The density of sources is therefore described as $\rho_S(\theta, \omega)$ and its variation represents the variation in the strength of surface-wave noise sources at different azimuths. The travel-time delay, $\Delta t \equiv \Delta t_d$, for a source at a given azimuth is given by eq. (2), which can be rewritten as

$$\Delta t(\theta) \equiv t(\xi) = \frac{\Delta x \cos\theta}{v} + \frac{\Delta x_{sx}}{v_{avg-sy-sx}} - \frac{\Delta x_{sx}}{v_{avg-sx}}, \tag{11}$$

where Δx is the station–station distance, v is the average velocity on the path to station y in excess of the distance to station x (see Fig. 1), $v_{avg-sy-sx}$ is the average velocity along the path shown in Fig. 1, and Δx_{sx} and v_{avg-sx} are as defined in Section 2.1. All velocities are potentially dispersive, with implicit dependence on ω. If

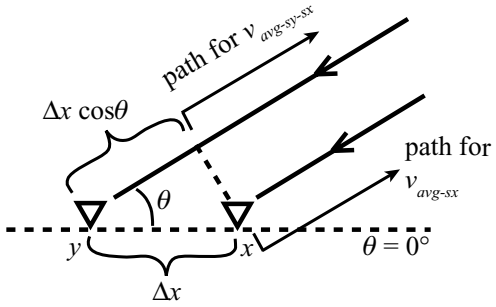

Figure 1. Schematic of the geometry considered. Stations x and y are separated by distance Δx, the long dotted line represents the great-circle path connecting the stations, θ is the azimuth of the noise source relative to the station–station path and the difference in distance from the source to the two stations is given by $\Delta x \cos\theta$ for a source located infinitely far away. The average velocity along the $\Delta x \cos\theta$ path is given by v and the remaining paths have average velocities $v_{avg-sy-sx}$ and v_{avg-sx} as shown.

velocity perturbations are relatively small and well distributed, or if Δx is relatively small compared to the length-scale over which large velocity changes occur, then the second and third terms of eq. (11) will tend to cancel out, leaving the first term as the dominant contribution. These assumptions can fail to be achieved in many realistic situations. (They would fail if the path Δx_{sx} samples a medium with a very different average velocity compared with that sampled by the path Δx_{sy}.) However, based on typical station–station spacing used in noise tomography studies and typical velocity variations in the frequency range of interest (e.g. Lin *et al.* 2008), both of these assumption are somewhat reasonable and will be assumed for the remainder of Section 2. Thus, here, we take

$$\Delta t(\theta) \approx \frac{\Delta x \cos\theta}{v}. \tag{12}$$

Note that if velocity structure is non-uniform, v will have a dependence on θ and could more appropriately be written $v \equiv v(\theta)$ (but will be assumed to be spatially uniform for the rest of this section). Rearranging eq. (12) yields

$$\xi(\Delta t) \equiv \theta(\Delta t) = \arccos\left(\frac{v\Delta t}{\Delta x}\right). \tag{13}$$

Substituting eq. (13) into eq. (9) for $\rho(\Delta t)$ yields

$$\begin{aligned}\rho(\Delta t) &= \rho_S(\theta(\Delta t)) \cdot \frac{v/\Delta x}{\sqrt{1-(v\Delta t/\Delta x)^2}} \\ &= \rho_S(\theta) \cdot \frac{v/\Delta x}{|\sin\theta|}.\end{aligned} \tag{14}$$

$\rho(\Delta t)$ is the quantity that determines how different noise sources are weighted in their contribution to the travel-time measurement of eq. (10). It therefore represents the sensitivity to a given physical distribution of sources ρ_S. Substituting eq. (14) into eq. (10) thus yields the desired result

$$\tau(\omega) = \frac{1}{\omega}\left\{\phi\left[\int \frac{W(t)\rho_S(\theta(t))v/\Delta x}{\sqrt{1-(vt/\Delta x)^2}} e^{i\omega t}\, dt\right] + 2\pi N\right\}, \tag{15}$$

that is the traveltime measured from a cross-correlation measurement of an arbitrary distribution of far-field surface-wave noise sources in a medium with a given velocity structure. (Note the dependence of ρ_S, ρ and v on ω is left implicit in eq. (14) and henceforth. The meaning of infinite density points will be discussed in Section 2.4.) See Fig. 2 for examples of various $\rho(\Delta t)$.

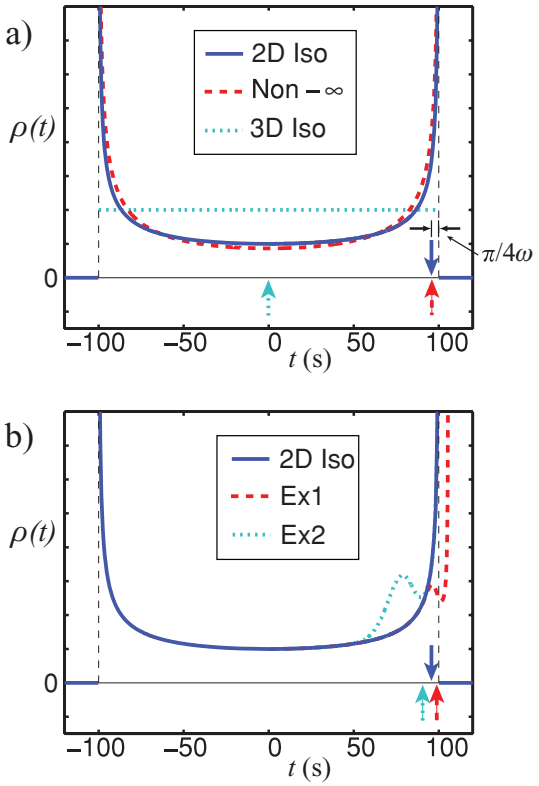

Figure 2. Density function versus travel-time delay, $\rho(t) \equiv \rho(\Delta t_d, \omega)$, plotted for different situations, all with a station spacing of 400 km and a uniform background velocity of 4 km s^{-1}. Since only phases are measured, absolute amplitudes shown are arbitrary. The coloured arrows along the zero-line denote the travel-time measurement (eq. 10) of the respective $\rho(t)$ at a period of 40 s and with a broad windowing function around the expected (positive) travel-time. (a) The blue solid line is for the 2-D isotropic case ('2-D Iso'); the red dashed line is for 2-D isotropic but sources a finite distance away ('Non-∞'); and the cyan dotted line is for the 3-D isotropic case ('3-D Iso'). The 'Non-∞' case is plotted using the approximation of eq. (17) with $r/\Delta x \approx 0.7$ and is re-normalized to make comparison easier. For $r/\Delta x \gtrsim 3$, the 'Non-∞' line would be indistinguishable from the blue line. The actual measured travel times are 94.8 s for '2-D Iso,' 95.0 s for 'Non-∞ and 0.0 s for '3-D Iso.' As expected from eq. (21), both '2-D Iso' and 'Non-∞' are shifted by close to $\pi/4\omega = 5$ s from the station–station travel time of 100 s. (b) The blue solid line, again, is the 2-D isotropic case for comparison; the red dashed line is for the -1 km s^{-1} perturbation case of the first example of Section 3 ('Ex1'); and the cyan dotted line is for the second example of Section 3 ('Ex2'). When the red and cyan lines cannot be seen, it is because they are indistinguishable from the blue line. The actual measured travel times are 96.8 s for 'Ex1' and 92.3 s for 'Ex2.'

When sources are not located infinitely far away from the stations but are instead at distance r, we can modify our results as follows. Treating $\Delta x/r$ as a small parameter and v as constant, we expand eq. (2) to include one higher-order term, yielding

$$\Delta t(\theta, r) \approx \frac{\Delta x}{v}\cos(\theta) \cdot \left[1 - \frac{1}{8}\left(\frac{\Delta x}{r}\right)^2 \sin^2\theta\right]. \tag{16}$$

It is clear from eq. (16) that as long as $r \gtrsim 5\,\Delta x$, the error introduced by using eq. (12) will be relatively minor, with an error to Δt of less than $1/(8 \cdot 5^2) \approx 0.5$ per cent. Since velocity perturbations of interest are also small, this approximation error may be important for sources very close to the stations (e.g. at $r/\Delta x = 2$ the error is as large as 3.1 per cent) and the effect can be accounted for indirectly by modifying the true density $\rho_S(\theta, r)$ so that it represents

an effective 'infinite distance' density $\rho_S(\theta) = M(\theta, r) \cdot \rho_S(\theta, r)$. For this transformation

$$M(\theta, r) = \left| \frac{\partial\theta(\Delta t, r)}{\partial \Delta t} \Big/ \frac{d\theta(\Delta t, \infty)}{d\Delta t} \right| = \left| \frac{d\Delta t(\theta, \infty)}{d\theta} \Big/ \frac{\partial \Delta t(\theta, r)}{\partial \theta} \right| \approx \left[1 - \frac{1}{8} \left(\frac{\Delta x}{r} \right)^2 (2 - \sin^2 \theta) \right]^{-1}, \quad (17)$$

with $\Delta t(\theta, r)$ being the travel-time delay at azimuth θ and distance r. Eq. (17) further shows that the effect of the multiplicative correction $M(\theta, r)$ is to enhance density in the vicinity of the station–station path ($\theta \sim 0$), which slightly helps to localize the cross-correlation peak (compare the solid blue and dashed red curves in Fig. 2a). If multiple distances r are represented, as is likely the case in the Earth, then the correction factor can be averaged over the distance range of interest,

$$\rho_S(\theta) = \int M(\theta, r) \rho_S(\theta, r)\, dr. \quad (18)$$

2.3 Derivation of the noise correlation property for isotropic surface-wave noise

Previous three-dimensional (3-D) results like those of Lobkis & Weaver (2001) and Roux *et al.* (2005) imply that the cross correlation $C_{xy}(t)$ is related to the (displacement) Green's function $G_{xy}(t)$ by

$$\frac{C_{xy}(t)}{dt} \equiv C'_{xy}(t) \approx -G_{xy}(t) + G_{xy}(-t) \quad (19)$$

and take a time derivative of the cross-correlation to arrive at an acausal Green's function. Since a time derivative is equal to multiplication by $i\omega$ in the frequency domain, this effectively results in a phase shift of $-\pi/2$ at each period. To obtain $G_{xy}(t)$ from the acausal Green's function, the result is then either averaged or (more commonly) the larger of the positive and negative signals is taken as representative. To go from the (e.g. vertical–vertical) Green's function $G_{xy}(t)$ to a surface-wave phase travel time, one performs a phase shift $\pi/4$ toward zero (a negative shift at positive t and vice versa) to account for the asymptotic far-field representation of the (2-D) surface-wave Green's function (Dahlen & Tromp 1998). The phase travel time is then given by the time delay at the peak of the narrow-band filtered signal at a given period (up to a phase shift of 2π). The multiple phase shifts (including a shift of π for the negative sign) result in a net $-\pi/4$ shift for negative t and $+\pi/4$ for positive t in going from the original cross-correlation to the phase travel time.

We now show that this net phase shift is approximately correct but that the theoretical motivations for this result within the literature (Sabra *et al.* 2005; Yao *et al.* 2006; Benson *et al.* 2007; Lin *et al.* 2008), whether based on eq. (19) or otherwise, are misleading. The essential reason that many previous derivations do not strictly apply to the travel-time measurement of surface waves is that they assume an isotropic incidence of the measured waves in 3-D, whereas surface waves are waves that inherently travel in 2-D since the third dimension (depth) is integrated out (and are waves due to sources primarily near the free surface). Since isotropic incidence of waves in 3-D does not imply the same noise correlation properties as isotropic incidence of waves in 2-D (see Section 2.5), derivations assuming 3-D isotropic noise do not apply to measurements of isotropic surface-wave noise. The surface-wave results of Snieder (2004) do not share this same problem but instead only apply in the infinite frequency limit and therefore cannot easily be interpreted when measuring waves with a given finite frequency, ω.

To properly understand why previous surface-wave studies have been able to obtain reasonable travel-time measurements, we apply the results of Section 2.2. Assuming v is spatially uniform, eq. (14) allows the distribution of noise sources in space to be mapped into a distribution of sources in travel-time delay. If the sources are randomly (isotropically) distributed in azimuth, then $\rho_S(\theta)$ is constant. Choosing for convenience a normalization of 1 over the interval $0 \le \theta \le \pi$, that is $\int_0^\pi \rho_S(\theta) d\theta = 1$, then $\rho_S = 1/\pi$ and eq. (14) yields

$$\rho(\Delta t) = \frac{v/\Delta x}{\pi |\sin\theta|} = \frac{v/\Delta x}{\pi \sqrt{1 - (v\Delta t/\Delta x)^2}}. \quad (20)$$

As shown in Appendix A, substituting eq. (20) into eq. (10) for $\tau(\omega)$ gives

$$\tau(\omega) \approx \frac{\Delta x}{v} - \frac{\pi}{4\omega} + \frac{2\pi N}{\omega} \quad (21)$$

for positive time delay and similarly

$$\tau(\omega) \approx -\left[\frac{\Delta x}{v} - \frac{\pi}{4\omega} \right] + \frac{2\pi N}{\omega}, \quad (22)$$

for negative time delay (also see Fig. 2). Thus, we obtain approximately the same $\pi/4\,\omega$ phase shift as previously found, but without the problems inherent in applying those results to travel-time measurements of surface waves. Eqs (21) and (22) apply strictly only in the same infinite frequency limit as in Snieder (2004), but eq. (A4) of the Appendix applies at all ω and one can easily compute the error accrued from the infinite frequency approximation, as plotted in Fig. 3(a) for a positive windowing function (see Appendix). This error, which is due to the errors in using the asymptotic approximations to the Bessel and Struve functions, is similar but not identical to the error in using a far-field approximation for traditional source–station tomography. As shown in Fig. 3(a), this error is significant for relatively long period (low frequency) waves and small station–station spacing (but depends on the windowing function used). For example, choosing $\Delta x = 100$ km, $v = 4$ km s^{-1} and $T \equiv 2\pi/\omega = 10$ s, would yield $\omega/(v/\Delta x) = 15.71$ and therefore a 0.9 per cent error in the travel-time measurement if the infinite frequency approximation were used. To our knowledge, no papers in the existing noise tomography literature account for this error, which can be comparable to the few percent variations in velocities that typically occur in the Earth. Most authors (e.g. Yao *et al.* 2006) simply throw away data for which station–station spacing is small rather than account for the correction suggested here. Including this data may improve tomographic resolution.

One may note that it has been pointed out by Nakahara (2006) that a Hilbert transform should be applied to the cross-correlation to obtain the (displacement) Green's function, but that step is unnecessary since the phase information has already been obtained without needing to calculate the Green's function as an intermediate step. One should also note that although group velocity studies (Shapiro *et al.* 2005; Benson *et al.* 2007; Cho *et al.* 2007; Yang *et al.* 2007) do not initially arrive at the phase travel time, they make group velocity measurements based on this same phase travel time and are therefore affected in the same way. In general, the group travel time can be expressed in terms of the phase travel time as

$$\tau_g(\omega) = \tau(\omega) + \omega \cdot (d\tau/d\omega). \quad (23)$$

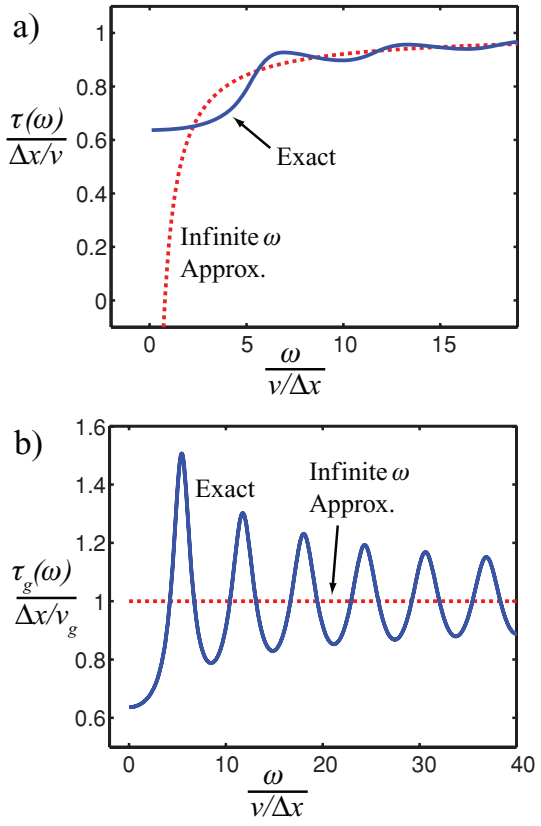

Figure 3. (a) Travel-time measurement $\tau(\omega)$ normalized by $\Delta x/v$ as a function of frequency ω normalized by $v/\Delta x$. The blue solid line is the exact result as given by eq. (A4) for a strictly positive (boxcar) windowing function. The red dotted line is the high frequency approximation given by eq. (21) that is equivalent to a phase shift of $-\pi/4\omega$ (for positive time delay). For both curves, it has been assumed that the $2\pi N/\omega$ phase ambiguity has been properly accounted for. (b) Group travel-time measurement $\tau_g(\omega)$ normalized by $\Delta x/v_g$ (where v_g is group velocity) as a function of frequency ω normalized by $v/\Delta x$. The blue solid line is the exact result calculated by substituting eq. (A4) (with the same positive windowing function) into eq. (23). The red dotted line is the high frequency approximation calculated by substituting eqs (21) into (23).

Interestingly, in the high frequency approximation (substituting eq. 21), the group travel time is then given by

$$\tau_g(\omega) \approx \Delta x/v \cdot (1 - \omega/v \cdot (dv/d\omega)) = \Delta x/v_g \qquad (24)$$

(for positive time delay), where v_g is group velocity and therefore does not have an apparent time shift due to the cross-correlation measurement. However, this lack of apparent time shift is not a feature of the general expression (using eq. A4 rather than eq. 21 to calculate τ_g), which has large deviations from $\Delta x/v_g$ as shown in Fig. 3b even when $\omega/(v/\Delta x)$ is relatively large. For example, choosing $\Delta x = 100$ km, $v = 4$ km s^{-1} and $T = 5$ s then $\omega/(v/\Delta x) \approx 31.4$ but there is still a $\approx$10 per cent error in assuming $\tau_g = \Delta x/v_g$. As for phase travel-time measurements, this error depends on the windowing function used.

2.4 An infinite frequency description

So far, we have discussed how noise correlation measurements can be made on waves of a given frequency. It is often useful from both a practical and pedagogical standpoint to consider the infinite frequency limit since the description is considerably simpler in this limit. Taking the limit as $\omega \to \infty$ of eq. (10) for $\tau(\omega)$, one immediately recognizes that if there exist infinite-density points of $\rho(\Delta t)$ in eq. (14) then these points completely determine the cross-correlation response of eq. (10) as these points effectively act as delta functions in picking out travel times. These infinite-density points correspond to stationary travel-time delay points, making this description analogous to a stationary-phase approximation description like that utilized by Snieder (2004). However, the relative simplicity of our approach allows quantitative examination of the conditions under which noise-correlation measurements give reasonable traveltime measurements. A few simple examples of this are now given.

When noise is isotropically distributed in 2-D, then ρ_S is constant and eq. (14) has infinite density points at $\theta = 0, \pi$ or equivalently $\Delta t = \pm\, \Delta x/v$, consistent with the limit as $\omega \to \infty$ of eqs (21) and (22). Thus, we immediately recover the result that the cross-correlation has a response at the (positive and negative) travel-time delay between the two stations.

In the framework of our formulation, the infinite-frequency cross-correlation measurement can fail to retrieve the expected station–station travel-time delay either because $\rho(\Delta t)$ achieves an infinite response at time delays other than $\Delta t = \pm\Delta x/v$ or because $\rho(\Delta t)$ achieves a less-than-infinite response at $\Delta t = \pm\Delta x/v$. These failures can occur due to a non-uniform source distribution $\rho_S(\theta)$ or due to a non-uniform velocity distribution $v(\theta, r)$. For example, if $\rho_S(\theta)$ drops to zero at $\theta = 0$ and $\theta = \pi$ then $\Delta t = \pm\Delta x/v$ may not have infinite $\rho(\Delta t)$ and the traveltime measurement will instead yield a value near the average Δt of $\rho(\Delta t)$ (or of $W(\Delta t)\ \rho(\Delta t)$ if a windowing function is used as well). On the other hand, the velocity distribution $v(\theta, r)$ can easily be such that $\Delta t(\theta)$ has multiple stationary points, thus giving additional Δt for which $\rho(\Delta t)$ is infinite. In these cases, one must take a limit of eq. (10) to determine which infinite values are most important.

2.5 Noise correlation for 3-D isotropic noise

Many previous authors have discussed the relationship between the cross correlation and the Green's function when noise is distributed isotropically in 3-D (Lobkis & Weaver 2001; Snieder 2004; Roux *et al.* 2005; Nakahara 2006). However, none of these descriptions addresses the case when this 3-D distributed noise is dispersive in nature (with different frequency waves travelling at different velocities) and more importantly they do not discuss whether meaningful travel times can be measured in this case. Although the dispersion of (3-D) body waves is less important than for (2-D) surface waves, at least a small amount of physical dispersion exists through the dispersive effects of attenuation and this fact makes it of interest to consider the case of dispersive 3-D distributed sources. Due to the different dimensionality, it will be shown that a very different conclusion must be made about the possibility of measuring travel times from standard noise correlation measurements when sources are distributed isotropically in 3-D (Unlike previous work, we only discuss implications for travel-time measurements and do not discuss implications for the related but different problem of Green's function reconstruction.).

Before continuing, the applicability of this 3-D isotropic description should perhaps be commented upon. Most sources of seismic energy occur near the surface (e.g. Snieder 2004; Kedar *et al.* 2008); scattering of seismic energy is thought to be more efficient in the near-surface heterogeneous lithosphere (e.g. Campillo & Paul 2003; Larose *et al.* 2006); and the increase of seismic velocities with depth effectively confines most seismic energy to (2-D) surface waves.

Thus, it is evident that most applications of seismic noise tomography are not well described by sources being evenly distributed in 3-D and these sources also do not excite the Earth's normal modes equally. The bulk of current noise tomography applications, including all applications that explicitly measure travel times of surface waves, are therefore much better approximated with the 2-D surface-wave description of Sections 2.2–2.4. However, there may be important applications in which noise sources are uniformly distributed in 3-D, especially in smaller-scale industrial applications where noise sources could potentially be placed in such a configuration.

For 3-D distributed far-field sources in a uniform velocity 3-D medium, the spatial density function $\rho_S(\boldsymbol{x}, \omega)$ can be written as $\rho_S(\theta, \phi, \omega)$ where θ is the polar angle and ϕ is the azimuth with respect to the station–station line. If, as in Section 2.2, we assume that eq. (12) applies, then the parametrization $\xi = \theta$ still works and we can again consider ρ_S parametrized as $\rho_S(\theta, \omega)$. For isotropic noise in this 3-D case, $\rho_S(\theta, \phi, \omega)$ is constant so that performing an integration over ϕ yields $\rho_S(\theta, \omega) = |\sin\theta|$. Substituting this into eq. (14) then shows that $\rho(t) \equiv \rho(t, \omega)$ is constant between $\pm\Delta x/v$ (see Fig. 2). Putting this $\rho(t)$ into eq. (10) shows that $\tau(\omega) = 0 + 2\pi N/\omega$, that is the standard noise-correlation traveltime measurement yields a travel time of zero and is therefore independent of any useful travel-time information (No window is used since all delay times between $\pm\Delta x/v$ contribute equally.). A group velocity measurement would similarly give a group time-lag of zero. If sources were not exactly isotropically distributed, then the region with slightly higher $\rho(t)$ would contribute more to the phasing and would result in a phase shift centred at this travel-time delay $t_{\rho+}$ (up to a $2\pi N$ phase shift). The travel time resulting from a phase velocity measurement would be $t_{\rho+}$; a group velocity measurement would yield the associated time delay $t_{\rho+} + \omega \cdot (dt_{\rho+}/d\omega)$. Thus, the travel-time curve resulting from both phase and group velocity measurements would have no relation to the velocity structure between the stations but would instead give information about the anisotropy of the source distribution. This analysis should caution the potential user of 3-D isotropic noise that if one wants to extract useful travel-time information, non-standard techniques for measuring phase or group travel times will be necessary. Again, it should be kept in mind that this section's analysis is for a uniform velocity 3-D medium in which surface waves are not important, a situation that does not obviously apply to the Earth.

3 EXAMPLES OF APPLYING THE NEW APPROACH

Perhaps the most important conclusion of Section 2 is that most of the sensitivity to phase travel time occurs close to the station–station line in the 2-D isotropic case, unlike the 3-D isotropic case where the sensitivity is strong away from the station–station line. Yet simply using the ray theory approximation, as done here, it is already the case that sensitivity to velocity structure is non-zero away from the station–station line (see Fig. 2) and this sensitivity accounts for the approximate $\pi/4$ phase shift toward zero in the 2-D isotropic case. Whereas some of this has been demonstrated in some recent numerical experiments (e.g. Lin *et al.* 2008; Yang & Ritzwoller 2008), no existing work demonstrates how to calculate this sensitivity without performing numerical experiments. It would be useful, for example, to calculate a phase sensitivity kernel as in traditional surface-wave tomography (e.g. Dahlen & Tromp 1998; Zhou *et al.* 2004). Unfortunately, since $\rho(t)$ is a function of the derivative of travel-time delay with azimuth and not the travel-time delay itself (see eq. 9), our approach shows that one cannot describe a phase travel-time perturbation as an integral over a kernel multiplied by velocity perturbations. However, since $\rho(t)$ gives the travel-time delay through eq. 10), $\rho(t)$ itself can be thought of as a sensitivity kernel. So, given a velocity distribution, one can express the travel-time delay t as a function of azimuth as in eq. (11), take the derivative, and arrive at $\rho(t)$ directly which then yields the phase travel time as described by eq. (10). For a noise source distribution far from 2-D isotropic, one must also perform analysis like that of Stehly *et al.* (2006) or Yao & van der Hilst (2008) to determine the distribution of sources to arrive at $\rho(t)$ as described by eq. (9). Using this forward modelling of the phase travel time iteratively with noise tomography results has the potential to enhance the accuracy and reproducibility of tomographic images derived from noise tomography. Even if the calculated corrections are small, quantifying the errors arising from a noise tomography approach would assuage concerns over the robustness of the derived images. Furthermore, the shapes of noise-tomography sensitivity kernels are different than standard finite-frequency kernels (e.g. Zhou *et al.* 2004) regardless of whether corrections are needed.

A simple example of this sensitivity slightly away from the station–station line is shown in Fig. 4. In this example, the stations are 400 km apart and the source distribution $\rho_S(\theta)$ is taken as constant. The velocity is uniformly 4 km s^{-1} except for a roughly Gaussian velocity perturbation, centred three quarters of the way from station 1 to station 2, with a maximum of $\Delta v_{\max} = -1$, 0 and $+1$ km s^{-1} (respectively) and length scale of 50 km (see Fig. 4a). Eq. (9) for $\rho(t)$ can be evaluated for this given velocity distribution by explicitly calculating $t(\xi) \equiv \Delta t(\theta)$ with eq. (2). Doing this numerically and substituting the result into eq. (10) with a broad (130 s) windowing function centred at positive delay time gives the phase travel time. Accounting for the approximate $\pi/4$ phase shift of eq. (21) expected of the isotropic case and then dividing the station–station distance by this phase-corrected travel time gives the average phase velocity between the stations (see Fig. 2b). If only the ray between the stations contributed to determining the phase velocity, the three cases would have average velocities of 3.79, 4.00 and 4.23 km s^{-1}, respectively and would be independent of period. Instead, as shown in Fig. 4(b), whereas the uniform velocity case ($\Delta v_{\max} = 0$) yields approximately the correct result (with small errors due to choice of windowing function, finite discretization of the time series, and the $\pi/4$ approximation), both non-uniform velocity cases yield phase velocities closer to 4 km s^{-1} than is predicted for sensitivity strictly on the station–station line and both cases have a significant period dependence even though the velocity structure in the example is non-dispersive. One should note that the discrepancy is worse for lower frequencies (longer periods) since these frequencies are more sensitive to a wider range of delay times, and thus more sensitive to structure away from the station–station line.

Another simple example is given that illustrates the sensitivity to an anisotropic noise source distribution. In this example, we again take the stations to be 400 km apart and the velocity is assumed to be uniformly 4 km s^{-1}. The source distribution is taken as $\rho_S(\theta) = 1 + 2\cos^{300}[(\theta - 40^\circ)/2]$ to represent a narrow, roughly Gaussian peak of sources around $\theta = 40^\circ$ superimposed on an isotropic distribution with half the strength (see Fig. 5a). As expected, the (phase-corrected) velocity measured is close to the expected result (4 km s^{-1}) for periods much shorter than the time delay $\Delta t_{40} \approx \Delta x\,(1 - \cos 40^\circ)/v \approx 23$ s, but is sensitive to the anisotropy at longer periods (see Fig. 5b). The increase in measured phase velocity at the long-period end is also expected since Δt_{40} is still comparable to the periods considered ($2\pi/\omega$). (At even longer periods than shown,

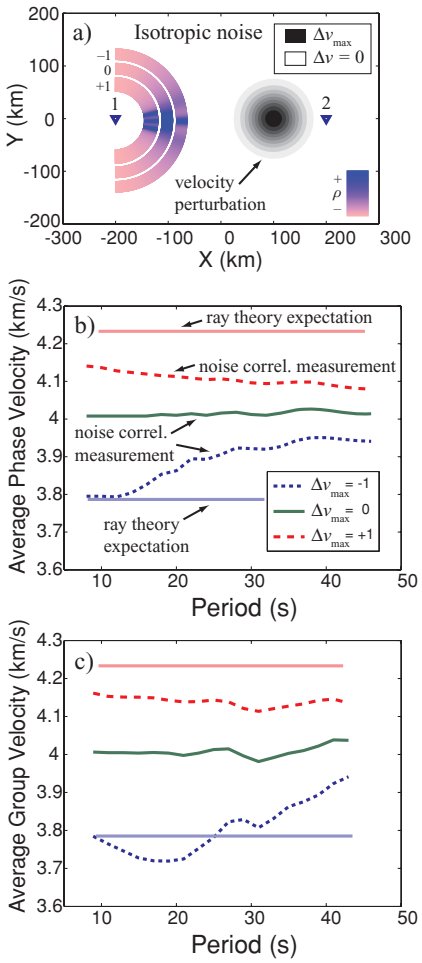

Figure 4. Example of phase and group velocities recovered in a non-uniform velocity medium. Panel (a) describes the geometry: the stations are triangles and the shading denotes the velocity perturbation away from 4 km s^{-1}. The coloured rings surrounding station 1 denotes the azimuthal sensitivity $\rho(t(\theta))$ for the positive time delay window for the three cases considered, with colours ranging from light red (not sensitive, low ρ) to dark blue (sensitive, high ρ). Panel (b) describes the average phase velocity measured from station 2 to station 1, for $\Delta v_{\max} = -1$, 0 and $+1$ (dotted blue, solid green and dashed red, respectively). The average phase velocity along the station–station path is 3.79, 4.00 and 4.23 km s^{-1}, respectively (as shown in matching faded lines). Whereas the average phase velocity for the uniform velocity closely approximates the expected value of 4.00 km s^{-1}, for both non-uniform velocity cases the velocities are different than the station–station path average. Panel (c) describes the average group velocity for the same configuration. Line colours and styles are as in panel (b). Since the example medium given is non-dispersive, the average group velocity along the station–station path is also 3.79, 4.00 and 4.23 km s^{-1}, respectively.

when $2\pi/\omega \gg \Delta t_{40}$, there is a small decrease in measured phase velocity due to the excess of sources within $|\Delta t| > \Delta x/v - \pi/\omega$ but this sensitivity drops as more unaffected regions are averaged over.) The decrease in measured phase velocity for intermediate period waves is perhaps a little counterintuitive, but is due to the excess of sources being at a time delay slightly less than $9\pi/4\omega$ (or $[1 + 2\pi N]/4\omega$ for any integer N) from $\Delta x/v$ and therefore shifting the measured phase travel time toward higher values.

It should be noted that the two examples were chosen to illustrate differences between ray-theoretical expectations and actual

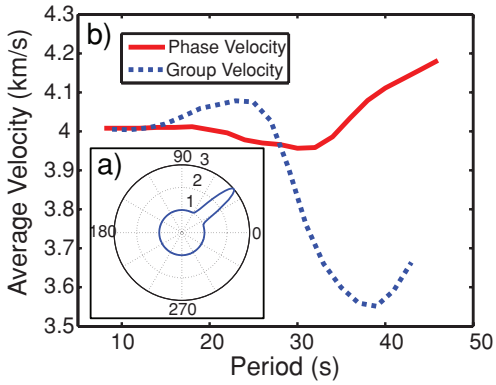

Figure 5. Example of phase and group velocities recovered when the source distribution is anisotropic. Inset (a) describes the noise source anisotropy, with $\rho_S(\theta)$ plotted in polar coordinates (with θ in degrees). Main panel (b) describes the average phase and group velocity measured around the expected (positive) travel time. Since the example medium is non-dispersive, the ray theory expectation is 4.0 km s^{-1}, independent of period.

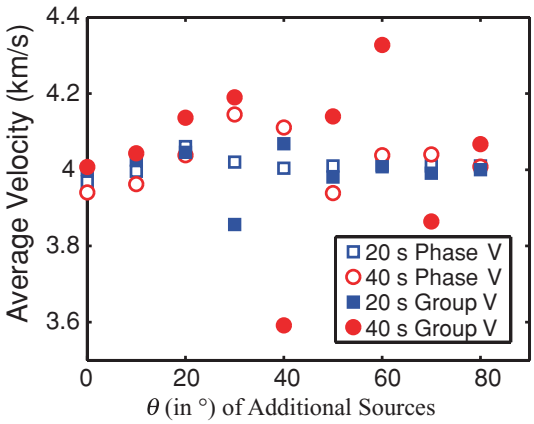

Figure 6. Example of 20 and 40-s phase and group velocities recovered when the source distribution is anisotropic like in Fig. 5 but with the additional sources at different azimuths, ranging from $\theta = 0°$ to 80°. As in Fig. 5, the example medium is non-dispersive and the ray-theory expectation is 4.0 km s^{-1}, independent of period and source distribution.

ray-theoretical measurement for cases that have significant differences. For many arbitrary distributions of noise sources and/or velocity structures, the differences are much smaller and therefore unimportant compared to other uncertainties in the measurements. For example, plotted in Fig. 6 are 20 and 40-s phase and group velocity measurements for the same anisotropic source distribution of the previous paragraph, except with anisotropy centred at different azimuths θ. Comparison of these curves shows that measurements for $\theta = 80°$ are much closer to the expected 4 km s^{-1} compared to measurements for $\theta = 30°$ or 40° and so would be unlikely to cause significant problems. However, the fact that the azimuth of the source anisotropy changes the measured travel times (at a given period) means that if source anisotropy is not correctly accounted for then it will be improperly mapped into anisotropic velocity structure.

The above conclusions apply equally well to group velocity studies as to phase velocity studies. The primary difference is that group velocity studies do not need to apply the $\approx\pi/4$ phase shift (see eq. 24). In spite of this, it is important to recognize that group velocities are just as much affected by the energy arriving (slightly)

away from the station–station line (see Figs 4c and 5b) that accounts for the $\approx \pi/4$ phase shift in phase travel time. When the calculated travel times are significantly different than expected, group velocity tomographic images should also be corrected for this sensitivity to velocity structure away from the station–station line.

4 CONCLUSIONS

We have presented a new, simple ray-theoretical derivation that describes the relationship between cross-correlations of seismic noise and the direct travel time measured between two stations. This new framework allows us to understand the travel-time measurement even when noise sources are potentially frequency-dependent, non-uniformly distributed and within a dispersive, non-uniform velocity medium. Applying this new framework is relatively straightforward and shows why noise tomography has been generally successful but also allows for quantification of the errors that arise in assuming isotropic noise sources, a uniform-velocity medium and infinite frequency waves. Using our approach, it is possible to correct for these factors. Since these corrections are not particularly computationally intensive, we suggest that future researchers should compute the corrections and implement them in areas where the corrections are significant. Doing this may, for example, allow a larger percentage of data to be useful than is currently used in most applications. Additionally, calculating these corrections, even if mostly negligible, would give seismic noise tomography results a more theoretically sound basis and alleviate fears traditional seismologists may have regarding the robustness of noise tomography-derived images.

ACKNOWLEDGMENTS

The author would like to thank C. A. Dalton, A. M. Dziewonski, M. G. Sterenborg, H. Kanamori, G. Ekström, H. Yao, M. Betancourt and J. R. Rice for helpful discussion and M. Ritzwoller and various anonymous reviewers for constructive criticism. The author also thanks editors J. Trampert and M. Diament. This research was supported by a National Science Foundation Graduate Fellowship.

REFERENCES

Aki, K., 1957. Space and time spectra of stationary stochastic waves, with special reference to microtremors, *Bull. Earthq. Res. Inst.,* **35,** 415–457.

Benson, G.D., Ritzwoller, M.H., Barmin, M.P., Levshin, A.L., Lin, F., Moschetti, M.P., Shapiro, N.M. & Yang, Y., 2007. Processing seismic ambient noise data to obtain reliable broad-band surface wave dispersion measurements, *Geophys. J. Int.,* **169,** 1239–1260.

Campillo, M. & Paul, A., 2003. Long-range correlations in the diffuse seismic coda, *Science,* **299,** 547–549.

Chavez-Garcia, F.J. & Luzon, F., 2005. On the correlation of seismic microtremors, *J. geophys. Res.,* **110**, B11313, doi:10.1029/2005JB003671.

Chavez-Garcia, F.J., Rodriguez, M. & Stephenson, W.R., 2005. An alternative approach to the SPAC analysis of microtremors: exploiting stationarity of noise, *Bull. seism. Soc. Am.,* **95,** 277–293.

Cho, K.H., Herrmann, R.B., Ammon, C.J. & Lee, K., 2007. Imaging the upper crust of the Korean peninsula by surface-wave tomography, *Bull. seism. Soc. Am.,* **97,** 198–207.

Claerbout, J.F., 1968. Synthesis of a layered medium from its acoustic transmission response, *Geophysics,* **33,** 264–269.

Cox, H., 1973. Spatial correlation in arbitrary noise fields with application to ambient sea noise, *J. acoust. Soc. Am.,* **54,** 1289–1301.

Dahlen, F.A. & Tromp, J., 1998. *Theoretical Global Seismology,* Princeton University Press, Princeton, NJ.

Derode, A., Larose, E., Campillo, M. & Fink, M., 2003. How to estimate the Green's function of a heterogeneous medium between two passive sensors? Application to acoustic waves, *Appl. Phys. Lett.,* **83,** 3054–3056.

Eckart, C., 1953. The theory of noise in continuous media, *J. acoust. Soc. Am.,* **25,** 195–199.

Ekström, G., Tromp, J. & Larson, E.W.F., 1997. Measurements and global models of surface wave propagation, *J. geophys. Res.,* **102,** 8137–8157.

Kedar, S., Longuet-Higgins, M., Webb, F., Graham, N., Clayton, R., & Jones, C., 2008. The origin of deep ocean microseisms in the North Atlantic Ocean, *Proc. R. Soc. A,* **464,** 777–793.

Kustowski, B., Ekström, G. & Dziewonski, A.M., 2008. Anisotropic shear wave velocity structure of the Earth's mantle: a global model, *J. geophys. Res.,* **113**.

Larose, E. *et al.*, 2006. Correlation of random wavefields: an interdisciplinary review, *Geophysics,* **71,** SI11–SI21.

Li, X.D. & Romanowicz, B., 1995. Comparison of global waveform inversions with and without considering cross-branch modal coupling, *Geophys. J. Int.,* **121,** 695–709.

Lin, F.C., Moschetti, M.P. & Ritzwoller, M.H., 2008. Surface wave tomography of the western United States from ambient seismic noise: Rayleigh and Love wave phase velocity maps, *Geophys. J. Int.*, **173,** 281–298.

Lobkis, O.I. & Weaver, R.L., 2001. On the emergence of the Green's function in the correlations of a diffuse field, *J. acoust. Soc. Am.,* **110,** 3011–3017.

Montelli, R., Nolet, G., Dahlen, F.A., Masters, G., Engdahl, E.R. & Hung, S.H., 2004. Finite-frequency tomography reveals a variety of plumes in the mantle, *Science,* **303,** 338–343.

Nakahara, H., 2006. A systematic study of theoretical relations between spatial correlation and Green's function in one-, two- and three-dimensional random scalar wavefields, *Geophys. J. Int.,* **167,** 1097–1105.

Ritsema, J., van Heijst, H.J. & Woodhouse, J.H., 2004. Global transition zone tomography, *J. geophys. Res.,* **109**.

Roux, P., Sabra, K.G., Kuperman, W.A. & Roux, A., 2005. Ambient noise cross correlation in free space: theoretical approach, *J. acoust. Soc. Am.,* **117,** 79–84.

Sabra, K.G., Gerstoft, P., Roux, P., Kuperman, W.A. & Fehler, M.C., 2005. Surface wave tomography from microseismcs in Southern California, *Geophys. Res. Lett.,* **32**.

Sanchez-Sesma, F.J. & Campillo, M., 2006. Retrieval of the green's function from cross correlation: the canonical elastic problem, *Bull. seism. Soc. Am.,* **96,** 1182–1191.

Sanchez-Sesma, F.J., Perez-Ruiz, J.A., Campillo, M. & Luzon, F., 2006. Elastodynamic 2-D Green function retrieval from cross-correlation: canonical inclusion problem, *Geophys. Res. Lett.,* **33**.

Shapiro, N.M. & Campillo, M., 2004. Emergence of broad-band Rayleigh waves from correlations of the ambient seismic noise, *Geophys. Res. Lett.,* **31**.

Shapiro, N.M., Campillo, M., Stehly, L. & Ritzwoller, M.H., 2005. High-resolution surface-wave tomography from ambient seismic noise, *Science,* **307,** 1615–1618.

Snieder, R., 2004. Extracting the Green's function from the correlation of coda waves: a derivation based on stationary phase, *Phys. Rev. E,* **69,** 1–8.

Snieder, R., Wapenaar, K. & Larner, K., 2006. Spurious multiples in seismic interferometry of primaries, *Geophysics,* **71,** SI111–SI124.

Stehly, L., Campillo, M. & Shapiro, N.M., 2006. A study of the seismic noise from its long-range correlation properties, *J. geophys. Res.,* **111,** 1–12.

Wapenaar, K., 2004. Retrieving the elastodynamic Green's function of an arbitrary inhomogeneous medium by cross correlation, *Phys. Rev. Lett.,* **93,** 1–4.

Wapenaar, K., Slob, E. & Snieder, R., 2006. Unified Green's function retrieval by cross correlation, *Phys. Rev. Lett.,* **97**.

Yang, Y. & Ritzwoller, M.H., 2008. Characteristics of ambient seismic noise as a source for surface wave tomography, *Geochem. Geophys. Geosyst.,* **9**, Q02008, doi:10.1029/2007GC001814.

Yang, Y., Ritzwoller, M.H., Levshin, A.L. & Shapiro, N.M., 2007. Ambient noise Rayleigh wave tomography across Europe, *Geophys. J. Int.,* **168,**

259–274.

Yao, H. & van der Hilst, R.D., 2008. Analysis of bias in surface wave phase velocities from ambient noise interferometry and an iterative approach for azimuthal anisotropy, *EOS, Trans. Am. geophys. Un.,* **89**(53), Fall Meet. Suppl., Abstract S31A-1897.

Yao, H., van der Hilst, R.D. & de Hoop, M.V., 2006. Surface-wave array tomography in SE Tibet from ambient seismic noise and two-station analysis, I. Phase velocity maps, *Geophys. J. Int.,* **166,** 732–744.

Zhou, Y., Dahlen, F.A. & Nolet, G., 2004. Three-dimensional sensitivity kernels for surface wave observables, *Geophys. J. Int.,* **158,** 142–168.

APPENDIX A: PROOF OF THE APPROXIMATE $\pi/4\omega$ PHASE SHIFT APPLICABLE TO SURFACE-WAVE NOISE TOMOGRAPHY

We take v to be spatially uniform but potentially dispersive, $t(\theta) = \Delta x \cos\theta / v$ and rewrite eq. (20) as

$$\rho(t(\theta)) \propto \frac{v/\Delta x}{\sqrt{1-(v\Delta t/\Delta x)^2}} = \frac{v/\Delta x}{|\sin\theta|}. \tag{A1}$$

For a positive windowing function

$$W(t) = \begin{cases} 1, & t > 0 \\ 0, & t < 0 \end{cases}. \tag{A2}$$

Eq. (10) thus simplifies to

$$\begin{aligned} \omega\tau(\omega) + 2\pi N &= \phi\left[\int_0^{\Delta x/v} \frac{v/\Delta x}{\sin\theta(t)} e^{i\omega t}\, dt\right] \\ &= \phi\left[\int_0^{\pi/2} e^{i\cos\theta\omega\Delta x/v}\, d\theta\right]. \end{aligned} \tag{A3}$$

The integral in eq. (A3) is identified as a Bessel integral, giving

$$\omega\tau(\omega) + 2\pi N = \phi\big[\alpha_1[J_0(\omega\Delta x/v) + i\,H_0(\omega\Delta x/v)]\big] \tag{A4}$$

where J_0 is a Bessel function of the first kind of order zero, H_0 is a Struve function of order zero and α_1 is a constant. Taking $\omega\Delta x/v \gg 1$, eq. (A4) can be approximated as

$$\begin{aligned} \omega\tau(\omega) + 2\pi N &\approx \phi\big[\alpha_1[J_0(\omega\Delta x/v) + i\,Y_0(\omega\Delta x/v)]\big] \\ &\approx \phi\left[\frac{\alpha_2}{\sqrt{\omega\Delta x/v}} \cdot \exp\left[i\left(\frac{\omega\Delta x}{v} - \frac{\pi}{4}\right)\right]\right] \\ &\approx \frac{\omega\Delta x}{v} - \frac{\pi}{4}, \end{aligned} \tag{A5}$$

where Y_0 is a Bessel function of the second kind of order zero and α_2 is a constant. Thus, for positive time delay

$$\tau(\omega) \approx \frac{\Delta x}{v} - \frac{\pi}{4\omega} + \frac{2\pi N}{\omega} \tag{A6}$$

and similarly, for negative time delay

$$\tau(\omega) \approx -\left[\frac{\Delta x}{v} - \frac{\pi}{4\omega}\right] + \frac{2\pi N}{\omega}. \tag{A7}$$

We therefore derive the approximate $\pi/4\omega$ phase shift between $\tau(\omega)$ (the phase delay as measured by noise-correlation techniques) and $\Delta x/v$ (the phase travel time in a homogeneous velocity medium) without calculation of the surface-wave Green's function. It may be noted that the 2-D surface-wave Green's function can be expressed in terms of J_0 and Y_0 so that comparison with eq. (A4) would result in an explicit relationship between noise-correlation measurements and the Green's function response, as in other works.